

## REVIEW ARTICLE OPEN

## Outlook for graphene-based desalination membranes

Albert Boretti<sup>1,2,9</sup>, Sarim Al-Zubaidy<sup>3</sup>, Miroslava Vaclavikova<sup>4</sup>, Mohammed Al-Abri<sup>5</sup>, Stefania Castelletto<sup>6,7</sup> and Sergey Mikhailovsky<sup>8</sup>

We discuss here next-generation membranes based on graphene for water desalination, based on the results of molecular simulations, application of nanofabrication technologies, and experiments. The potential of graphene to serve as a key material for advanced membranes comes from two major possible advantages of this atomically thin two-dimensional material: permeability and selectivity. Graphene-based membranes are also hypothetically attractive based on concentration polarization and fouling, and graphene's chemical and physical stability. Further research is needed to fully achieve these theoretical benefits, however. In addition, improvement in the design and manufacturing processes, so to produce performance and cost-effective graphene-based desalination devices, is still an open question. Finally, membranes are only one part of desalination systems, and current processes are not optimized to take full advantage of the higher selectivity and permeability of graphene. New desalination processes are, therefore, needed to unlock the full benefits of graphene.

npj Clean Water (2018)1:5; doi:10.1038/s41545-018-0004-z

## INTRODUCTION

Membranes for water purification and water desalination are being used more and more to address global challenges of pollution and scarcity of water.<sup>1</sup> Highly selective and high-permeable next-generation membranes are proposed to address the limitations of the current membrane technologies. Molecular-level design approaches are becoming popular toward fabricating these membranes, and graphene derivatives are among the most promising of those novel materials.<sup>2</sup>

Graphene was first observed in electron microscopes in 1962 supported on metal surfaces.<sup>3</sup> It was rediscovered in 2004 by Novoselov and Geim.<sup>4</sup> They were awarded the Nobel Prize in Physics 2010<sup>5</sup> "for groundbreaking experiments regarding the two-dimensional material graphene". Since 2010, graphene has attracted a growing interest for many applications including desalination. Lockheed Martin patented in 2013 the graphene-based membrane for water desalination "Perforene".<sup>6</sup> This nanoporous membrane is made of a thin graphene sheet that is perforated with nanometric holes.

Graphene comprises carbon atoms that are bonded together in hexagonal patterns. Mono-layered and double-layered graphene is so thin that it can be considered a two-dimensional material. Graphene's flat honeycomb pattern gives it many amazing characteristics. It is one of the strongest, lightest, most conductive, and transparent materials. The single layers of carbon atoms provide the basis for many other materials. Graphene oxide (GO) is an oxidized graphene derivative, which is less expensive and easier to produce. Graphene cannot be used as a separation membrane being hydrophobic and impermeable to water. The more hydrophilic GO serves as a basis for nanomembranes

impermeable to impurities, salts, or bacteria but permeable to water.<sup>7</sup>

GO is obtained by oxidation of graphite, which is then dispersed in basic solutions to produce GO.<sup>8,9</sup> It comprises single atomic layers of graphene with oxidized functional groups in its structure but mainly on the edges of graphene sheets.<sup>10,11</sup> Graphite oxide is composed of C, O, and H atoms. The ratios of C, O, and H in graphite oxide is variable. GO can be synthesized by several basic methods such as Brodie<sup>8</sup> or Hummers<sup>9</sup> and the many variations of these basic methods. Improvements are sought to achieve higher yield of GO using less expensive processes. Several composites have been obtained by mixing GO with polymers and other materials. This is done to improve such properties as conductivity, tensile strength, or elasticity of materials or simply to design new structures. Thin flat GO structures that can be folded, stretched, or wrinkled are obtained by attaching GO flakes one to another.

## Membrane processes

Relevant membrane processes for water purification and desalination include microfiltration (MF), ultrafiltration (UF), nanofiltration (NF), reverse osmosis (RO), membrane distillation (MD), ion exchange membranes, and forward osmosis (FO). The separation principle in these processes are mainly based on the different sizes of molecules and other objects (MF, UF, and NF), ionic charge of molecules, and membrane surface (NF, FO, and RO), hydrophobicity (MD), and electrical polarity (ion exchange membranes). MF, UF, NF, and RO are well-established processes in which separation is driven by a hydraulic pressure. FO is an emerging process in which separation is driven by an osmotic pressure. The osmotic pressure is the hydrostatic pressure applied on the salt side of the

<sup>1</sup>Department of Mechanical and Aerospace Engineering, Benjamin M. Statler College of Engineering and Mineral Resources, West Virginia University, Morgantown, WV 26506, USA; <sup>2</sup>Military Technological College, Muscat 111, Sultanate of Oman; <sup>3</sup>The University of Trinidad and Tobago, Wallerfield, Trinidad and Tobago; <sup>4</sup>Institute of Geotechnics, Slovak Academy of Sciences, Kosice 04001, Slovakia; <sup>5</sup>Sultan Qaboos University, Muscat 123, Sultanate of Oman; <sup>6</sup>School of Engineering, RMIT University, Bundoora, VIC 3083, Australia; <sup>7</sup>Swinburne University of Technology, Centre for Microphotonics, Hawthorn VIC 3122, Australia and <sup>8</sup>College of Life, Health and Physical Sciences, University of Brighton, Brighton BN2 4GJ, UK

Correspondence: Albert Boretti (a.a.boretti@gmail.com) or Sergey Mikhailovsky (sergeymikhailovsky@gmail.com)

<sup>9</sup>Present address: Independent scientist, Bundoora, VIC, Australia

Received: 18 January 2017 Revised: 21 August 2017 Accepted: 11 September 2017

Published online: 24 May 2018

membrane required to stop the water flow through a membrane. In RO, if pressures greater than the osmotic pressure are applied to the salt side of the membrane, water flows from the salt solution to the water side of the membrane.

MF and UF membranes are porous. MF membranes remove suspended particles and microbial pathogens. UF membranes remove macromolecules such as natural organic matter and smaller pathogens and biotoxins. UF membranes have molecular weight cutoff, the solute size at which 90% of species is rejected, ~5–500 kDa. Molecular separation in MF and UF membranes is based on a sieving or size exclusion mechanisms. NF membranes remove scale-forming ions, for instance, calcium and magnesium. NF membranes partially reduce salinity. NF membranes have molecular weight cutoffs of ~100–300 Da. Separation in NF membranes is based on a combination of sieving and solution-diffusion mechanisms. RO and FO membranes are used for desalination. Presently, RO and FO membranes are non-porous. Nearly all ions are removed by these membranes. Solutes without a charge having molecular weight greater than ~100 Da are also removed. The solution-diffusion model<sup>2</sup> controls the molecular transport in RO and FO membranes.

Graphene-based membranes are mostly intended for NF, RO, and FO. The advantages of graphene stem from the potentially very small thickness of the membrane and the highly controlled patterns of holes of very small diameters and small distances between holes. The mass transfer through the NF, RO, and FO graphene membranes may be described by the hydrodynamic model<sup>2,7</sup> or the solution-diffusion model.<sup>2</sup> Both models may be realized in real membranes.<sup>3</sup> The operation of graphene-based membranes is, however, only partially explained by these two simplified models.

In the hydrodynamic model,<sup>2</sup> the volumetric water flux through porous and non-porous membranes  $J_w$  is proportional to the hydraulic pressure drop across the membrane  $\Delta P$  and the osmotic pressure gradient across the active layer  $\Delta\pi$  with proportionality factor the water permeability of the RO literature  $A$ :<sup>7</sup>

$$J_w = \frac{D_w \cdot K_w^L \cdot c_{w0} \cdot v_w}{l \cdot R \cdot T} \cdot (\Delta P - \Delta\pi) = A \cdot (\Delta P - \Delta\pi) \quad (1)$$

In the above equation,  $D$  is the diffusion coefficient,  $K^L$  the medium coefficient,  $c_0$  the initial concentration of the bulk,  $v$  the molar volume,  $l$  the membrane thickness,  $R$  the gas constant, and  $T$  the temperature.<sup>7</sup> The salt flux  $J_s$  is given by the simplified formula<sup>7</sup> now involving the salt permeability constant  $B$  of the RO literature:<sup>7</sup>

$$J_s = \frac{D_s \cdot K_s^L}{l} \cdot \Delta c_s = B \cdot \Delta c_s \quad (2)$$

In the above equation,  $\Delta c_s$  is the solute concentration difference.

The performances of a RO membrane are typically given in terms of  $A$  and  $B$ .<sup>7</sup>  $\Delta\pi$  is the fundamental parameter of RO and FO membranes, while in MF and UF membranes  $\Delta\pi$  is negligible.

In porous membranes, the water permeability  $A$  may simply be approximated<sup>2</sup> as directly proportional to the product of surface porosity  $\varepsilon$  by the squared pore radius  $r_p$ , and inversely proportional to the product of solution viscosity  $\mu$  by active layer thickness  $\delta$ . Therefore,<sup>2</sup>

$$J_w = \frac{\varepsilon \cdot r_p^2}{8 \cdot \mu \cdot \delta} \cdot (\Delta P - \Delta\pi) = A \cdot (\Delta P - \Delta\pi) \quad (3)$$

The rejection of solutes present in the feed may then be approximated by an empirical function of the ratio of solute radius to pore radius  $a/r_p$ , with complete rejection achieved when  $r_p \leq a$ .<sup>12</sup>

The solution-diffusion model<sup>2</sup> applies to non-porous membranes where water and solute molecules separate into the active layer of the membrane, diffuse through the membrane polymer matrix down their chemical potential gradients, and desorb into the permeate solution. Solubility and diffusivity define the

diffusive permeability of water  $P_w$  and solute  $P_s$  that are intrinsic material properties independent of thickness. The water permeability  $A$  may be approximated<sup>13</sup> as directly proportional to the product of diffusive permeability of water  $P_w$  by molar volume of water  $V_w$ , and inversely proportional to the product of active layer thickness  $\delta$  by universal gas constant  $R$  by temperature  $T$ :

$$J_w = \frac{P_w \cdot V_w}{T \cdot R \cdot \delta} \cdot (\Delta P - \Delta\pi) = A \cdot (\Delta P - \Delta\pi) \quad (4)$$

The solute transport  $J_s$  is finally taken proportional<sup>13</sup> to the solute concentration gradient across the active layer  $\Delta c_s$ , with proportionality factor the solute permeability  $B$ , ratio of diffusive permeability of solute  $P_s$ , and active layer thickness  $\delta$ :

$$J_s = \frac{P_s}{\delta} \cdot (\Delta c_s) = B \cdot (\Delta c_s) \quad (5)$$

## Graphene-based membranes

Graphene-based membranes have been the subject of many recent literature reviews<sup>2,14–20</sup> that summarize some of the key performance parameters of graphene-based membranes. These reviews mostly highlight the benefits of high permeability and selectivity. These reviews also cover materials science aspects of the membranes, and molecular transport studies of the membranes.

Graphene is among the most promising materials for next-generation membranes in ref. <sup>2</sup> The lack of control over the permeability of water and solute is one significant limitation of membranes' performances. Fouling control is another key performance parameter that the new materials must, but not necessarily will address, as high separation performances may hardly be coupled to enhanced fouling resistance. Increased fouling and/or chemical resistance is a central area of concern in addition to permeability and selectivity.

The role of ultrahigh-permeability RO membranes for future membranes in desalination is further emphasized in ref., <sup>14</sup> however also indicating the need of new processes.

Extraordinary permeation properties coupled to additional properties such as antifouling, antibacterial, and photo degradation of nanomaterial-based membranes, including nanoparticles, nanofibers, two-dimensional layer materials, and other nanostructured nanomaterials and their composites, are promoted in ref.<sup>15</sup>

The importance of designing materials with rigid, engineered pore structures for selectivity and permeability is underlined in ref.<sup>16</sup> Scalability to practical modules is also shown to be critical for membrane materials screening.

All types of graphene membrane fabrication methods, specifically in form of a porous graphene layer, assembled graphene laminates and graphene-based composites, are discussed in ref.<sup>17</sup> This review evidences the large amount of work done in the past in conventional composite membranes, where graphene has been combined with polymers and ceramics to improve their mechanical properties.

Graphene and GO membranes and detailed proof of principle in both theoretical and experimental domains, for application in gas and water selections, are reviewed in ref.<sup>18</sup> The current defects in the graphene sheets such a grain boundary are shown to be relevant in determining their reliability in actual desalination plants as these defects can compromise the mechanical and selectivity properties attributed to graphene membrane. The operating conditions, such as pressure, temperature, and flux rate, which affect membrane selectivity, are however still to be determined. Reference<sup>18</sup> suggests to combine these ultrathin membranes with other porous membranes and methods already in use for pretreatment of mixture to avoid fouling and quick degradation of the graphene membranes. The same crucial parameters of these membranes such as pore size and interlayer spacing are still to be determined in practical examples as in combination with current membranes. Industrial applications are

shown to be challenging, as currently scalability is not up to the level to match industrial standards.

The fabrication and understanding of mass transport mechanism in nanoporous and GO laminates is reviewed in ref. <sup>19</sup> This review concludes on the superiority of both graphene and GO membranes over state-of-art polymer and ceramics-based membranes in terms of mass transport.

Reference<sup>20</sup> finally provides details of the excellent properties of graphene and GO freestanding and supported membranes as well as their fabrication methods for water desalination membranes. It is also evidenced that graphene and GO membranes can be less prone to fouling than other membranes. The challenges shown in this case are nanoporous controlled formation, to improve the mechanical performance of fully wetted nanoporous graphene (NPG) and GO membranes and determine whether transport mechanisms across NPG and GO nanosheets is charge or size-selective, large scale production of mechanically stable NPG and GO, balance between the fouling rejection and flux decline.

From these reviews, it may be concluded that the performance enhancement in the specific of high permeability and high selectivity are the most intuitive and proven advantages of graphene-based membranes. Robustness in the specific of mechanical, thermal and chemical stability, clean ability, and fouling resistance, remains an open question yet unresolved. Commercial readiness supported by manufacturing scalability, material and fabrication costs, and quality assurance/control are yet to be considered for practical applications.

After a brief report on the latest achievements in graphene-based membranes to complement the previously reviewed information, this contribution will discuss with a systemic approach the current outlook of graphene-based membranes especially in RO applications, being this a central, widespread, low-energy method for water desalination.

## GRAPHENE-BASED DESALINATION MEMBRANE TECHNOLOGY UPDATE

Graphene-based desalination membranes have been proposed mostly as NPG and graphene-based frameworks. Both forms serve as selective layers and operate as molecular sieves with size-based exclusion of undesired solutes. Other ideas are also being explored based on graphene. This other section is included to briefly discuss these other opportunities. In addition to the above membranes, it must be mentioned that GO are also commonly blended into porous membranes or used in the substrates for dense membranes. As the main concern of the paper is to discuss the opportunities of a high-permeability high-selectivity two-dimensional material, the vast literature on this aspect is not included in the current review.

### Nanoporous graphene

The simplest graphene-based desalination membrane can be produced by making nanoscale pores in a layer of graphene. This results in a flexible, chemically and mechanically stable separation membrane, based on a single-atomic layer thick material with target use in desalination. Water in fact can penetrate these subnanometer size pores, while salt ions larger than water molecules cannot and because of the ultralow thickness of the membrane, NPG was predicted<sup>21</sup> to have greater water permeability coefficients than current thin-film composite RO membranes (Fig. 1). Complete salt rejection was predicted<sup>21</sup> to be possible for hydroxylated pores of diameter 0.45 nm. Such performances were achieved for a 5  $\mu\text{m}$  diameter sample of NPG. The material was obtained by oxygen plasma etching of graphene grown through chemical vapor deposition (CVD).<sup>22</sup> Scaling up of NPG membranes is extremely challenging,<sup>2,22–26</sup> because it requires the formation of a large area of a single-layer, defect-free, graphene, and the scalable formation of uniformly sized nanopores.<sup>2</sup>

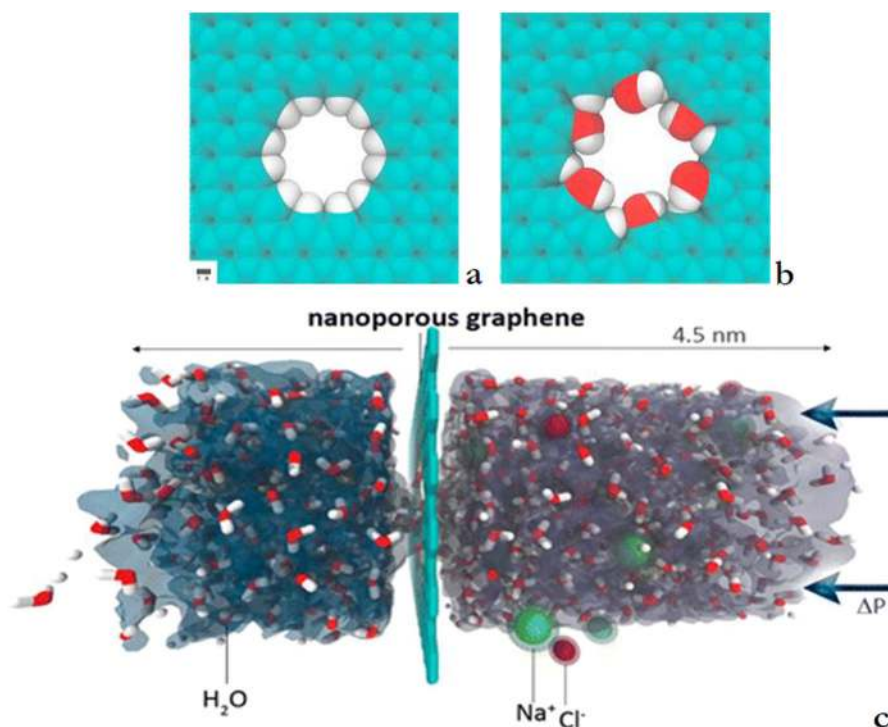


**Fig. 1** Model of (a) hydrogenated graphene pores, (b) hydroxylated graphene pores, and (c) complete computational system of ref. <sup>21</sup> (Images reprinted with permission from ref. <sup>21</sup> Copyright 2012 American Chemical Society)

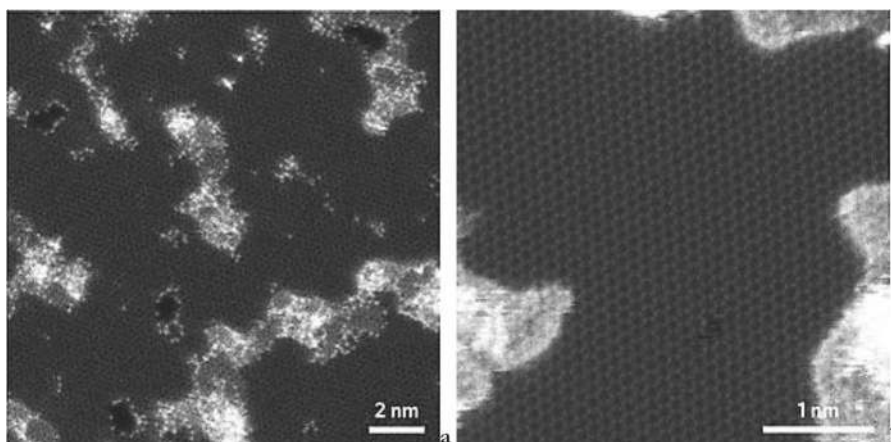


**Fig. 2** Scanning transmission electron microscope (STEM) images of graphene exposed to oxygen plasma for 1.5 s from ref. <sup>22</sup> The images are aberration-corrected. Pores have characteristic dimensions of  $\sim 1$  nm (Images reprinted from ref. <sup>21</sup> by permission from Macmillan Publishers Ltd, copyright 2015)

Single-layer graphene using CVD on a copper foil acting as catalyst, where single-layer carbon atoms can be formed, while growth conditions provide grain boundaries of graphene domains of  $50 \mu\text{m}$  in the final graphene sheet, were obtained at ambient pressure in ref. <sup>22</sup> To be used as a membrane for desalination, the graphene sheet needs to be transferred to a substrate, which is in this case made of silicon nitride, with a hole of  $5 \mu\text{m}$ . The actual graphene membrane is its suspended portion of  $5 \mu\text{m}$  diameter. The transfer can inflict damage to the membrane so a final electron microscopy imaging is required to determine whether any tear resulted after transfer or grain boundaries were falling within the  $5 \mu\text{m}$  hole, yielding 70% likelihood of intact membrane on the substrate. To create porous graphene, the membrane was then exposed to an oxygen plasma etching process to remove carbon atoms from the lattice, with larger and higher density of pores achieved with a longer exposure to the plasma. Defects were also introduced into single-layer unspoiled graphene by bombarding it by Ar ions with 3 keV energy and density of  $10^{15}$  ions  $\text{cm}^{-2}$  to remove approximately one to two atoms of carbon, thus creating nucleated pores.<sup>12</sup> This was followed by continuous 80 keV electron beam irradiation to enlarge the pores between 0.5 and 10 nm. However, while Ga ions and electrons with various energies were used in addition to plasma etching in ref.,<sup>22</sup> oxygen plasma-etching process allowed a control on the size of the pores and a final water transport, not observed in pores generated only by ion or electron beams (Fig. 2). The membranes with different plasma-etching exposure time (thus different pore size and concentration) were tested in terms of water and ion transport and compared to pristine graphene to determine the best nanofabrication conditions. It has been found in the specific case of ref. <sup>22</sup> that the higher density of pores considered resulted in a better membrane, provided the mechanical stability was not compromised, yielding the best performance with a density of pores of  $\sim 10^{12} \text{cm}^{-2}$ , and pore size of  $0.5 \div 1$  nm. The NPG membrane with lowest-defect density exhibits a nearly 100% salt rejection rate while maintaining a rapid water transport of up to  $10^6 \text{g m}^{-2} \text{s}^{-1}$  at  $40^\circ\text{C}$  driven by a hydraulic pressure difference. This water transport value is very high, as water fluxes driven by osmotic pressure difference were less than  $70 \text{g m}^{-2} \text{s}^{-1} \text{bar}^{-1}$ . This latter is  $\sim 7 \times 10^{-15} \text{g s}^{-1} \text{bar}^{-1}$  per pore, assuming a density of pores of  $10^{16} \text{m}^{-2}$ .

The first attempt to fabricate a membrane larger than micron size and thus closer to practical applications was made in ref.<sup>24</sup> A single layer  $25 \text{mm}^2$  CVD graphene was used to fabricate a graphene composite membrane obtained by transferring a single-layer commercial CVD graphene on a 200-nm commercial porous polycarbonate track-etched membrane. This membrane, in fact,

adheres to graphene on copper by simply applying pressure, and it is used as support for subsequent etching of the copper and further handling of the composite membrane. However, the transfer methodology and etching was found to be relevant to the final properties of the graphene composite membrane. Graphene pores were based on intrinsic defects or defects formed during processing without any further oxygen plasma etching or ion irradiation. The pressure-driven convection of water through the composite membrane and the bare polycarbonate track-etched membrane were compared, indicating a water flow reduction for the composite membrane corresponding to an 88–93% of graphene coverage. While measuring diffusion of KCl through the composite and bare membrane, it was found that the composite membrane was permeable to KCl. Intrinsic defects would allow transport of molecules smaller than the membrane pore sizes. The low-frequency presence of intrinsic 1–15 nm diameter pores is suggested in the CVD graphene.

The potential of practical use of single-layer graphene membrane is determined by the ability to create controllable subnanometer pores on a pristine graphene layer over a macroscopic area, and determine the molecular transport properties vs. the pore sizes. In ref.<sup>25</sup> isolated defects were first nucleated into the lattice of CVD graphene through initial Ga ion bombardment with acceleration voltage of 8 kV and density of  $6 \times 10^{12}$  ions  $\text{cm}^{-2}$ , and subsequently enlarged by chemical oxidative etching based on acidic potassium permanganate. The final permeable pores had the diameter of  $0.40 \pm 0.24$  nm after 60 min of chemical etching (the diameter did not increase at longer etching time). This pore size is required to guarantee selectivity of molecule separation while still maintaining high water permeability. The pores' density, however, increased with etching time, after 120 min approaching the theoretical limit of 80% of the ion fluence of  $6 \times 10^{12} \text{cm}^{-2}$ , which is close to the limit of a structural integrity of the graphene sheet that remained intact (Fig. 3). It was demonstrated that both ion bombardment and chemical etching were necessary to obtain the correct density and pore sizes. This method of fabrication of controlled size and density of nanopores was applied to the graphene composite membrane.<sup>24</sup> First, the composite membranes were fabricated and then subjected to Ga ion bombardment. Then, at different stages of in situ chemical etching, transport measurements of a dye and KCl were performed. When no etching was applied, some transport of KCl and the dye molecules was observed at the same level as for non-bombarded composite membrane, after 5 min etching the transport of KCl increased while the transport of dye molecules remained constant. The membrane potential also increased, indicating the membrane selectivity toward potassium



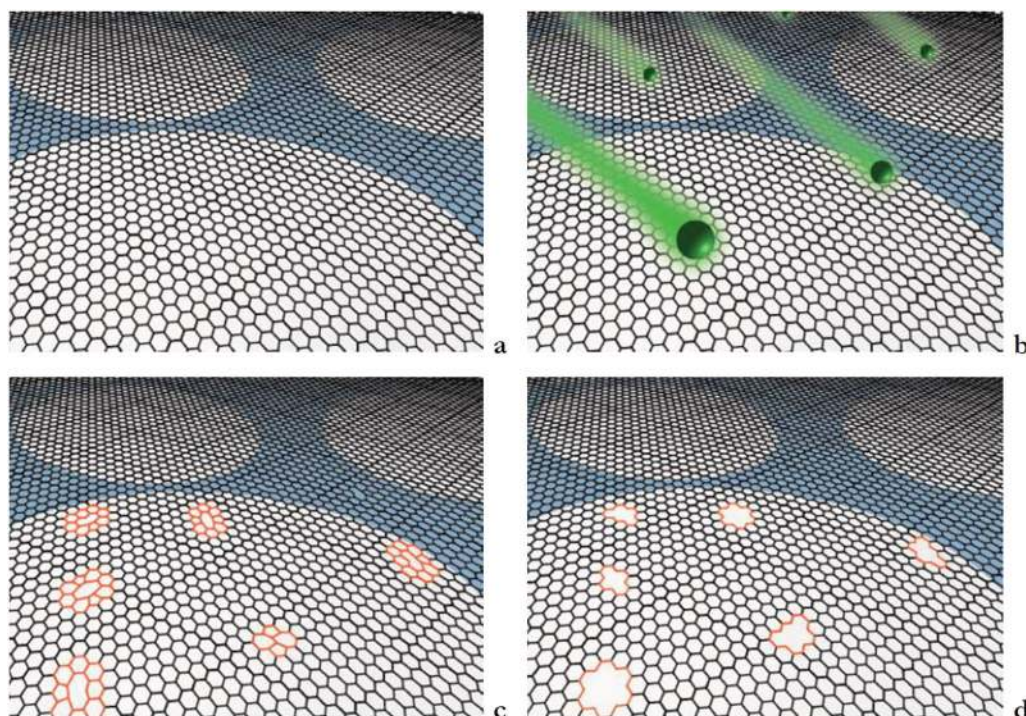


**Fig. 3** Process adopted in ref.<sup>25</sup> to create subnanometric pores of controlled shape in a layer of graphene. The unspoiled graphene (**a**) is subjected to ions bombardment with gallium ions (**b**) that generates reactive defect sites (**c**). Exposure to acidic potassium permanganate etchant completes the nanopores (**d**). (Figures reprinted adapted with permission from ref.<sup>25</sup> Copyright 2014 American Chemical Society)

cations compared to the chloride anions, most likely due to electrostatic interaction with functional groups formed at the pore edges. After 25 min etching the KCl transport remained constant and the membrane potential neutral, indicating that in enlarged pores no electrostatic effects were present due to removal of charged functional groups from pore edges, originated typically during short oxidation process. With longer etching time the dye transport started increasing, becoming again constant after 50 min etching. After 120 min etching both KCl and dye transport were identical to the polycarbonate track-etched membrane used as a support for the graphene composite membranes.

The fabrication of graphene composite membranes with a single layer of graphene on centimeter-scale needs careful processing to avoid to create tears and extrinsic defects (100–200 nm) in the final device, through which leaking can occur. In addition, intrinsic defects (1–15 nm) from the growth process sizes are present, limiting the efficacy of subnanometer controlled pore fabrication and the practicability of their application. As both transfer and growth are challenging to improve to reduce uncontrollable defects in the membrane, a multiscale sealing process has been proposed in ref.<sup>26</sup> As the defect size distribution is quite broad, a two-step sealing process has been proposed. For nanometer size, intrinsic defects and grain boundaries' atomic layer deposition with hafnia ( $\text{HfO}_2$ ) is used to fill the defects, as hafnia resists dissolution in both acidic and basic solutions. For larger extrinsic defects an interfacial polymerization reaction is used relying on nylon plugs that are formed only in larger tears and holes, efficiently sealing the remaining defects. By applying these two sealing methods to graphene composite membranes, the flux of KCl through such a membrane was reduced from 65 to 8% compared to the flux across a bare polycarbonate track-etched membrane. As an untreated graphene composite membrane, should be in principle impermeable to KCl, this residual 8% leakage is due to unsealed defects too large for hafnia deposition and too small for polymerization. This sealing process thus permits to create as results a centimeter-sized

membrane separating two fluids but with still a consistent amount of single-layer graphene membrane. The sealed graphene composite membranes were then ion-bombarded and subjected to chemical etching to form pores with a mean diameter of 0.162 nm and a tail extending to 0.5 nm. Such pores are expected to be water-permeable and impermeable to salt with diameters from  $\sim 0.275$  to  $\sim 0.7$  nm.<sup>26</sup> Water transport and solute rejection under FO were tested for the membranes. Water transport under forward osmosis was like current RO membranes used for water desalination. While the membranes rejected 70% of  $\text{MgSO}_4$ , 90% of allura red dye and 83% of dextran, NaCl transport was possible, being attributed to the residual unsealed defects.<sup>26</sup> Better details including the sizes of the solute species, if needed, are provided in the cited reference.

#### Graphene-based frameworks

Graphene-based framework membranes differ from NPG membranes in morphology and by water transport mechanism. They basically comprise multilayered graphene-based sheets,<sup>27–30</sup> or their functionalized derivatives (Fig. 4).

Although single-layer NPG membranes have shown potential as a RO desalination membrane,<sup>21</sup> their practicality is limited because of the lack of robustness required for real-world applications. The possibility to design multi-layer NPG membranes with improved characteristics for the same application was studied using molecular dynamic simulations in ref.<sup>27</sup> As per the authors, the synthesis of multi-layer NPG membranes is more economical than the production of single-layer membranes, and the novel membranes may be further tuned to enhance the separation processes. Multi-layer NPG membranes may have similar desalination properties as single-layer membranes. In addition, the separation processes may be further enhanced by optimizing the parameters describing the stacking of layers upon each other. The model represents a bi-layer membrane with given radius of the nanopores, separation of the layers, and offset of the pores in one layer and the other. The simulations provide guidance for the

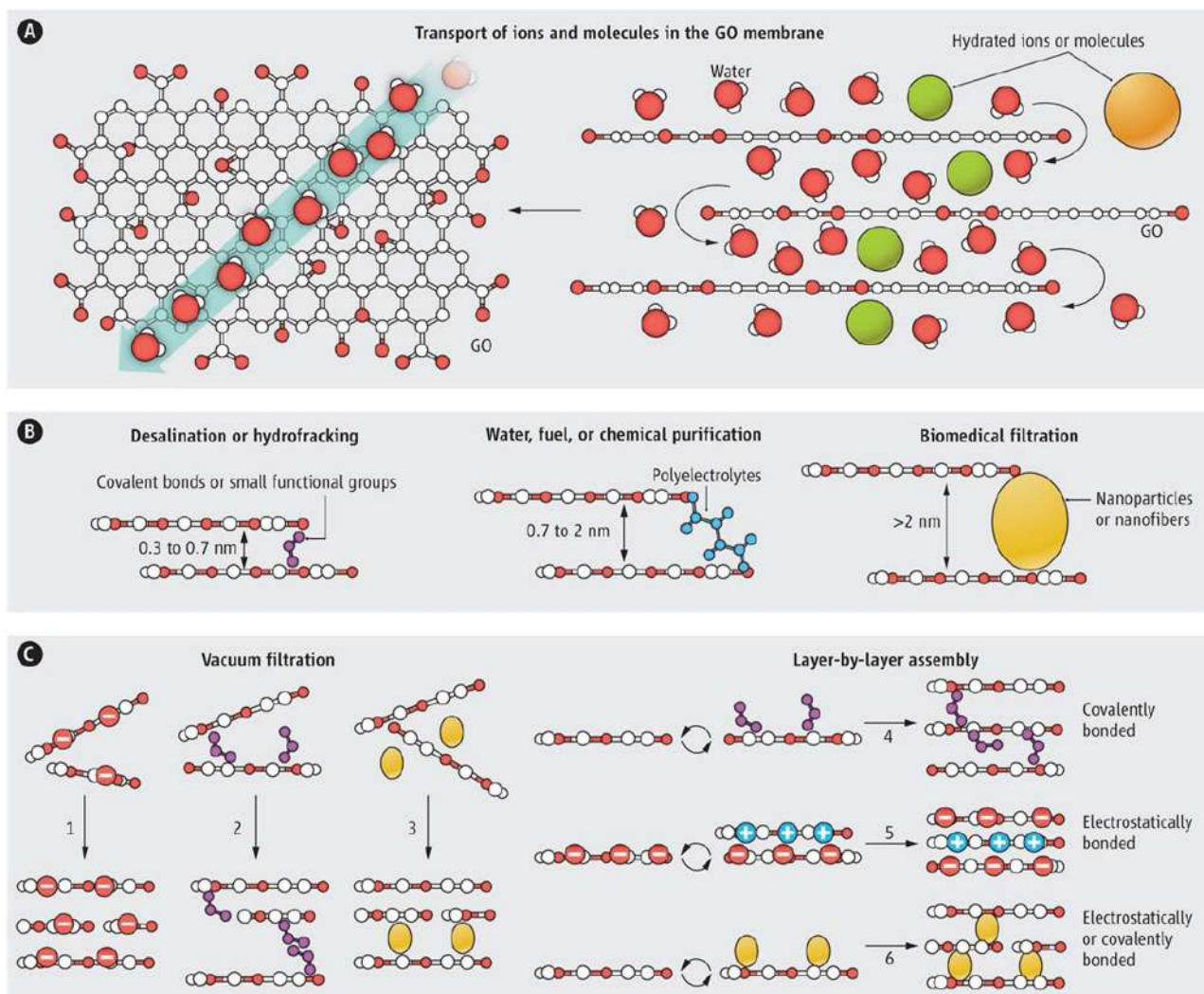


**Fig. 4** Graphene-based framework membranes from ref. <sup>30</sup> **a** Schematic of transport of ions and molecules in the membrane. **b** Tuning of the nanochannel size. **c** Methods for assembly, vacuum filtration or layer-by-layer assembly. (Image from ref. <sup>30</sup> reprinted with permission from AAAS.)

design of the multi-layer NPG membrane. This multi-layer approach has been applied more extensively to GO laminates as they are easier to fabricate via a more amenable industrial method known as vacuum filtration, thus with a better practical application potential. They are often referred to as GO Framework (GOF). GO-laminated membranes can be produced also by layer-by-layer deposition of GO. In ref. <sup>28</sup> these laminates were made of functionalized graphene sheets with an eventual micrometer thickness and an interlayer separation, which allows transportable layers of water through capillary pressure, regardless of the graphene hydrophobicity. GO was obtained from natural graphite flakes of millimeters' size, oxidized in concentrated potassium permanganate, sulfuric acid, and sodium nitrate, exfoliated by sonication in water, and then centrifuged to remove the few residual crystals. The GO-laminated membranes were fabricated from the GO suspension using vacuum filtration by anodic alumina membranes with 0.2  $\mu\text{m}$  pore diameter, 60  $\mu\text{m}$  length, and  $\approx 50\%$  porosity. The anodiscs were also used as mechanical support to GO membranes, as they were confirmed as irrelevant to the overall water permeation. The thickness of the GO membranes was controlled by varying the volume of the GO suspension from 0.5  $\mu\text{m}$  to more than 10  $\mu\text{m}$  thickness. The GO laminate membrane, while initially in a dry state, once immersed

in water, acts as a molecular filter. Solutes with radius larger than 0.45 nm are blocked. This was achieved by creating one-atom-wide graphene capillaries by piling layers of GO on top of each other. The cutoff is determined by the layers' separations. Thin laminate membranes were proved to be impermeable to all gases and vapors, except for water. In general, graphene-based frameworks allow ultrafast permeation of water, possibly because of the slip flow along the atomically smooth, non-oxidized graphene channels.<sup>29</sup> Once immersed in water, the laminate membrane slightly enlarges still allowing ultrafast flow of a few monolayers of water. Small salts with a size of less than 0.9 nm can flow along but larger ions or molecules are blocked.

Specifically, GOF membranes with 5  $\mu\text{m}$  thickness<sup>28</sup> were applied to verify water and other liquids, and ion permeation rates vs. molecular concentration over about 1  $\text{cm}^2$  area. Smaller ions permeate across the membranes at faster rates than expected for simple diffusion; thus, this effect has been attributed to anodisc effects. Critical to this result is the spacing between adjacent sheets, which increased from  $0.9 \pm 0.1$  nm in humid air to  $1.3 \pm 0.1$  nm when immersed in water, thus resulting in rapid permeation of ions.<sup>28</sup> One drawback is that graphene-based frameworks<sup>2</sup> show a sharp size-dependent cutoff too large for



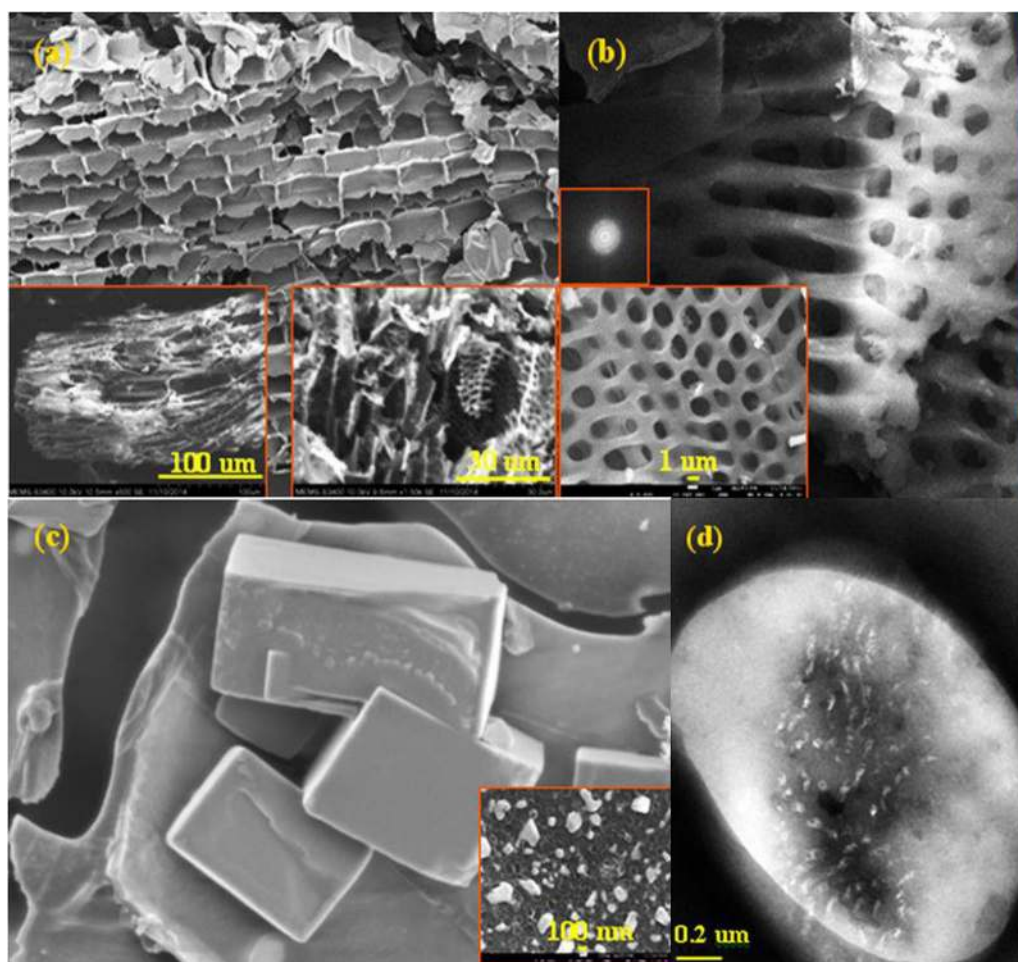


**Fig. 5** Microstructural analysis of porous membranes fabricated from 3D oxidized graphene framework from ref. <sup>37</sup> **a** Cross-sectional SEM micrograph of graphene-based filter showing micropores. Bottom-left inset shows micrograph of large chunk, while the bottom-right inset shows a zoomed-in image of a part of the same. **b** SEM micrograph view of a lower dimensional microhole array inside larger microhole structure. Inset on the left shows the front surface of similar such structure. **c** Large (~10 μm) NaCl crystallites sticking on the membrane after filtration. The inset at the bottom-left shows smaller (<200 nm) NaCl crystals on the surface of membrane. **d** TEM micrograph of clusters of NaCl nanocrystals on membrane (Images reproduced modified after ref. <sup>37</sup> Article distributed under a Creative Commons CC-BY license)

desalination and are generally unstable in water, unless they are stabilized by trace multivalent cations.<sup>31</sup>

To finely tune the membrane permeability, thus making them highly permeable to selected compounds and ions, it is necessary to modify the membrane channels. Specifically, for desalination the interlayer spacing needs to be decreased and their stability increased. This can be achieved by chemical or thermal reduction consisting in removing oxygen species. Using a full reduction of the GO membranes, the interlayer spacing is decreased to 0.36 nm, this separation being too small for allowing water flow between sheets. This limits water permeation to defect-driven flow.<sup>32</sup> Although a reduced GO (RGO) membrane was recently shown to allow water permeation with high-salt retention when tested in FO, the defect-driven permeation in this approach limits water permeability.<sup>33</sup>

As the GO sheets are enriched of numerous oxygen-containing functional groups (mainly hydroxyl and carboxyl groups), that allow GO to be easily exfoliated in solution, they can also be used to induce other chemical reactions resulting in additional functional groups. These additional groups can, for instance, permit GO layers to be interposed or crosslinked with primary complex monomers, or covalently linked with polymers. These properties have been used to provide another method for controlled decreasing of the interlayer spacing of laminar GO

membranes or GOF membranes, also contributing to the increasing of their overall stability due to covalent bonding.<sup>30,34,35</sup>

Diamine monomers were used in ref.<sup>34</sup> for crosslinking GO sheets to form laminar GOF membrane with a spacing between layers varying between 1.04 and 0.87 nm. These membranes were used to demonstrate dehydration of a mixture of water and alcohol by pervaporation and they provided a better long-term operation stability, owing to the suppression of the stretching of the sheet separation, by the solution absorbed in the membranes. However, these membranes have not shown any better salt rejection. The performance of GOF membranes made of cross-linkers, for water desalination and filtration of other contaminants such as bacteria, was assessed by classical molecular dynamics simulations.<sup>36</sup> By fine-tuning the GOF structure it is possible to remove all the ions from saltwater surpassing currently used RO membranes in regards of rate of salt separation. This can be achieved by using water-repellent graphene as part of the porous membrane as water is faster diffused in the attempt to avoid being in contact with graphene.

3D GOF membranes of ~1.2 cm diameter were synthesized from sugar cane bagasse using thermal processing and oxidizing graphene.<sup>37</sup> These porous membranes are complex 3D structures of oxidized graphene arranged in random piled style (Fig. 5). The result is an intricate path to assist in filtration through micro-

sieving and nano-sieving processes. Nano-sieving incorporated within the larger micro-sieving frameworks is proposed to desalinate and purify seawater from salts and pollutants such as  $\text{Cl}^-$  and  $\text{Na}^+$  ions, microbial pollutants, and dyes. Micro-sieving is achieved through the microchannels in the frameworks that stop larger suspended solids and bacteria. Further details of the membrane including size of pores may be inferred from the microstructural analysis of the porous membrane in Fig. 5 or the cited reference.

The synthesis of GO laminate membranes is challenging in establishing methods for the fine control of the interlayer of GO laminate within subnanometer range. This fine control is essential for precise sorting of small molecules.

A bottom-up approach was used in ref. <sup>38</sup> to create subnanometer 2D channels within GO layers and combining them with polymers to assembly GO layers with distance between layers of  $\sim 0.4$  nm and slit-like pores with size from 0.72 to 0.79 nm. First, single-layer GO nanosheets were prepared by chemical oxidation of bulk graphite. The self-assembly of these GO layers with subnanometer channels is achieved by exploiting "inner" forces from molecular interactions that are applied inside the laminate and "outer" forces derived from compressive, centrifugal, and shear forces, which are applied outside GO laminate during the fabrication process. The external forces are directing the GO layers piling to produce via plane-to-plane interlayers and in-plane slit-like pores, thus constituting a GOF with subnanometer in-plane channels. These GOFs with 2D channel membranes gave excellent performance in gas-sieving with  $10^2$ – $10^3$  higher  $\text{H}_2$  permeability and 300% better  $\text{H}_2/\text{CO}_2$  selectivity of commercial membranes.

A method to produce graphene-based NF membranes of large area was proposed in ref. <sup>39</sup> The membrane is obtained from discotic and nematic liquid crystals (LCs) of GO that are shear aligned. LC formation has been suggested as the best approach to produce self-assembled periodic materials from oriented graphene sheets.<sup>40</sup> Single-layered highly soluble GO sheets may indeed exhibit nematic liquid crystallinity in water.<sup>40</sup> The membrane is made by using a newly developed viscous form of GO finely and lightly spread with a blade.<sup>39</sup> The methodology is claimed to be faster while permitting larger sizes. The discotic nematic phase of GO is shear aligned to form ordered, continuous, thin films of multilayered GO on a support porous membrane. The method permits to produce relatively large-area membranes ( $13 \times 14 \text{ cm}^2$ ) in a reduced time frame of less than 5 s. By applying a pressure difference to the membrane, more than 90% of charged and uncharged organic probe molecules of hydrated radius above 0.5 nm are retained. Monovalent and divalent salts are also retained but only for a modest 30–40%. The obtained permeability is  $71 \pm 5 \text{ l m}^{-2} \text{ h}^{-1} \text{ bar}^{-1}$  ( $1.97 \pm 0.14 \times 10^{-10} \text{ m s}^{-1} \text{ Pa}^{-1}$ ) for  $150 \pm 15$  nm thick membranes. Solvent cleaning shows good flux recovery.

Sulfonation followed by mild reduction is proposed in ref. <sup>41</sup> to prepare well separated RGO laminate composite membranes. The method permits hydrophilic areas and interlayer spacing of 0.63 and 0.74 nm for ion selectivity and water permeation. Stability of the RGO film in water is then obtained by using in situ crosslinking reaction. They obtained fluxes to trans-membrane pressure of 61.7 LMH ( $\text{l m}^{-2} \text{ h}^{-1} \text{ kPa}^{-1}$ ), i.e.,  $1.71 \times 10^{-8} \text{ m s}^{-1} \text{ Pa}^{-1}$ . As common in ion exchange membranes, the selectivity is due to Donnan equilibrium and exclusion. They achieved rejections 80.5%  $\text{Na}_2\text{SO}_4$ , 52.0%  $\text{NaCl}$ , and 13.7%  $\text{MgCl}_2$  that are promising.

#### Other graphene-based membranes

The fabrication and morphology tuning of GO nanoscrolls (GONS) visualized as a GO sheet rolled into an open spiral wound structure has been discussed in ref. <sup>42</sup> Their synthesis is carried out via low- and high-frequency ultrasound solution processing

techniques of individual layers of GO. The scrolling activation energy for the formation of GONS is provided by the ultrasound handling. Ultrasound frequency, power density, and treatment duration determine their dimensions. Each GONS could be tailored to trap-specific molecules and pollutants, while by stacking billions of them layer by layer, they may be used to form a water purification membrane.

Single-layer graphene can transfer hydrogen protons.<sup>43</sup> While proton transfer through ideal single-layer graphene to occur requires overcoming large-energy barriers, when nanoscale holes or dopants are present or a potential bias is applied, this process can however become favorable under certain conditions. On the basis of simulations, naturally occurring defects such as missing carbon atoms can allow hydrogen protons to cross the barrier. It has been shown that protons transfer reversibly from the aqueous phase across the graphene via four-carbon vacancies, which were hydroxyl-terminated. These defects are creating water channels through the membrane.

A new diffusion mechanism for water molecules in motion on graphene surface has been revealed by molecular dynamics simulations.<sup>44</sup> On graphene water nanodroplets are moved by propagating nanoripples with a faster diffusion than their random motion on another material surface.

A "bilayered biofoam" for production of steam driven by the sun energy has been proposed in ref. <sup>45</sup> The novel membrane is made of a layer of bacterial nanocellulose (BNC) and a layer of RGO-filled BNC. The biofoam has a solar thermal efficiency of  $\sim 83\%$  under  $10 \text{ kW m}^{-2}$  simulated illumination. In the membrane, the top is the RGO-filled nanocellulose layer absorbing solar energy, and the bottom is the unspooled nanocellulose layer. The top layer is warmer. The heat transfer to the bulk water underneath is minimized by the bottom layer. The layers are permeable. The water filtering to the top surface evaporates. The cellulose of the bottom layer acts as a sponge, drawing water up to the GO of the top layer. The GO flakes are simply added to the medium where the bacteria for the cellulose are cultivated. The GO flakes get embedded in the layers of nanocellulose produced by the bacteria. The authors believe that this fabrication method is scalable and cost-efficient.

A fundamental work based on molecular dynamics simulations studied the ion separations of  $\text{NaCl}$  in aqueous solution.<sup>46</sup> The system studied consisted of two graphene nanosheets with one pore each, one being functionalized by fluoride (negatively charged) and the other by hydrogen atoms (positively charged). When an external electric field was applied to the system the fluoride pore and the hydrogen pore showed preferential selectivity toward  $\text{Na}^+$  and  $\text{Cl}^-$ , respectively; in addition, the higher the electric field, the faster is the movement of the ions from the salty water. The calculations of the potential of mean force for ions showed that sodium and chloride ions encountered an energy barrier, and thus, both cation and anion failed to permeate across the H-pore or F-pore of the GNS, respectively. On the basis of the results of this research, the functionalized GNS, as a membrane, can be suggested as a device in the field of water desalination.

#### PRESENT OUTLOOK FOR GRAPHENE-BASED DESALINATION MEMBRANES

There is a general agreement that next-generation membranes need to be highly selective, with high permeability to selected molecules, while also being inexpensive and sufficiently stable. The idea behind making membranes from GO is to use a very thin but strong and stable material with tiny, calibrated flow passages to provide high flow rates of water while collecting impurities targeting different sizes down to extremely small. One layer of graphene is only 335 picometers thick, and if grown on substrates such as silicon carbide, it may be everything between 85 and 415



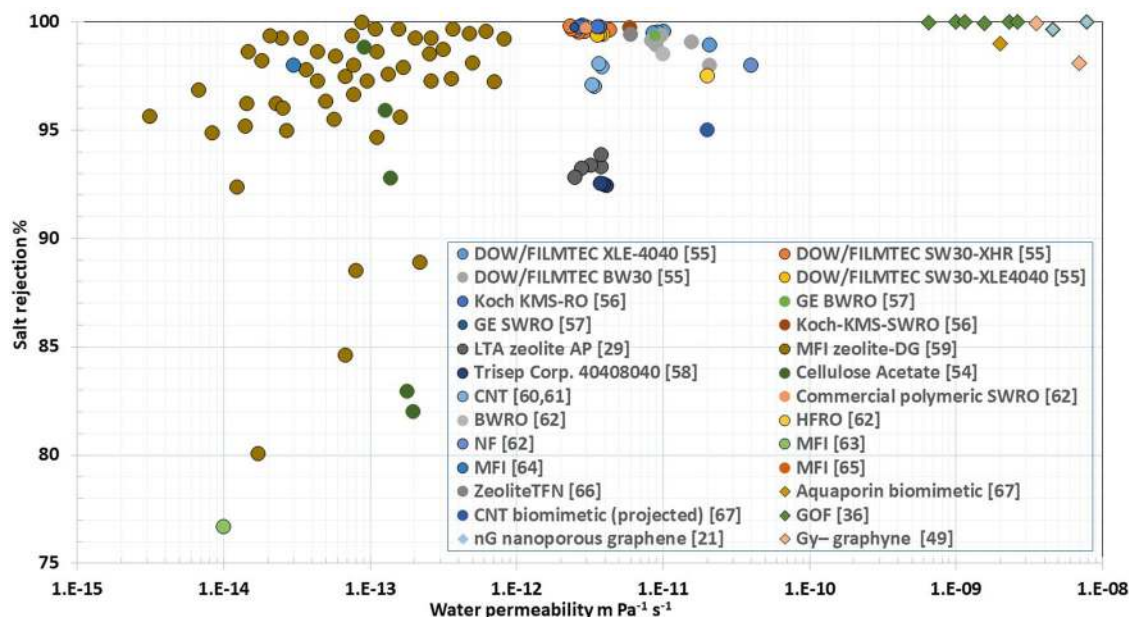


**Fig. 6** Comparison of permeability and salt rejection of commercial RO membranes and nanostructured membranes operating in seawater/high-salinity conditions and brackish/low-salinity conditions.<sup>29, 54–68</sup> TFN thin-film nanocomposite, CNT carbon nanotube, MFI zeolites, SWRO seawater reverse osmosis, BWRO brackish reverse osmosis, HFRO high-flux water reverse osmosis, NF nanofiltration. Results for GOF,<sup>36</sup> nG nanoporous graphene,<sup>21</sup> and Gy graphyne<sup>49</sup> are also included in the graph. Graphene-based RO desalination membranes have the potentials to deliver nearly complete salt rejection with permeability of  $\sim 10^{-9}$  m Pa<sup>-1</sup> s<sup>-1</sup>; however, this is only part of the story. Data of ref.<sup>54</sup> are also presented in ref.<sup>70</sup>

picometers.<sup>47</sup> Immaculate sheets of graphene are virtually impermeable to atoms and molecules. With pores of up to the subnanometer size, graphene can potentially act as a high selectivity and permeability filter only allowing to pass across the molecules smaller than the pores.

We reported on the fundamental lines of work proposing basic simulations at nanoscale and molecular levels, nanotechnologies to fabricate graphene-based membranes, and basic experiments performed on nanometer-size samples. Scaling up of the processes certainly requires further research. Production of sheets of high-quality material satisfying all the requirements of industrial membranes without complex and expensive processes appears to be extremely challenging. NPG, graphene-based frameworks, and other graphene-based membranes permit many different designs realizing different separation mechanisms and certainly qualify as one preferred candidate for future desalination membranes. Graphene is only one of the opportunities being considered for ultrathin-film membranes. The list of the other promising materials includes graphyne,<sup>48–50</sup> covalent triazine frameworks,<sup>51</sup> MoS<sub>2</sub>,<sup>52</sup> and boron nitride.<sup>53</sup>

Figure 6 summarizes the current state-of-the-art performances of hydrophilic commercial and hydrophobic laboratory membranes.<sup>21,29,36,49,54–68</sup> This subject is also covered in ref.<sup>69</sup> Hydrophilic commercial membranes exhibit excellent selectivity (>98% salt rejection) with relatively low permeability ( $2 \times 10^{-12}$ – $5 \times 10^{-12}$  for seawater and  $6 \times 10^{-12}$ – $2 \times 10^{-11}$  m Pa<sup>-1</sup> s<sup>-1</sup> for brackish water), while hydrophobic laboratory membranes show very high permeability ( $2 \times 10^{-10}$  m Pa<sup>-1</sup> s<sup>-1</sup>) but poor selectivity (50–60% salt rejection). Results for GOF,<sup>36</sup> nG nanoporous graphene,<sup>21</sup> and Gy graphyne<sup>49</sup> are also included in the graph. Graphene-based RO desalination membranes have the potentials to deliver nearly complete salt rejection with permeability better than  $10^{-9}$  m Pa<sup>-1</sup> s<sup>-1</sup>. However, other criteria must be satisfied to correctly rank these membranes against conventional RO desalination membranes.

Designing a new hydraulic pressure-driven membrane to achieve optimized practical membrane filtration, one must

address “three legs” or major criteria that underpin all membrane processes:<sup>70</sup>

- (i) selectivity
- (ii) permeability
- (iii) concentration polarization and fouling. But, also relevant are:
- (iv) chemical stability
- (v) physical stability
- (vi) economical cost
- (vii) environmental cost
- (viii) overall cost-to-benefit ratio.

As clearly the first two criteria could be satisfied, once scalability could be achieved, it is yet totally unexplored whether concentration polarization and fouling could degrade graphene-based membrane permeability and robustness.

As one example, it is important to consider the implications of membrane surface chemistry and flux on membrane fouling. Hydrophobic membranes offer high permeability, but may not sustain initially high values in the presence of organics in the feed having high affinity for such surfaces. This contrasts with more hydrophilic membranes normally exhibiting less severe organic fouling. High flux membranes will inevitably lead to increased concentration polarization and fouling, which will ultimately limit the process. In conventional RO membrane fouling mitigation strategies based on chemical and/or physical pretreatment of water, chemical modification of the membranes and periodic cleaning have been fully developed, while for the here proposed membrane it is yet unknown whether the same strategies could be applied or rather other strategies need to be developed to incorporate them in a desalination plant.

It may be further argued that an improved permeability not necessarily will deliver significantly better performances within current RO desalination systems. There are doubts on the possible performance benefits, as concepts such as the thermodynamic restriction of refs.<sup>70–75</sup> and minimum work of separation that applies to RO desalination drastically limit the benefits of higher permeability. Over the past two decades, there has been a

significant drop in the energy needed for RO desalination, and the present values of energy needs are already very close to the theoretical minimum for recovering salt-free water from seawater. On the basis of state-of-the-art seawater RO membranes, the specific energy consumption is  $\sim 2.2$  kWh/m<sup>3</sup>, which is hardly above the minimum work of separation at 50% recovery of  $\sim 1.8$  kWh/m<sup>3</sup>. Therefore, a more permeable membrane can only improve the energy demand, which is  $\sim 40\%$  of the total cost of seawater desalination by  $\sim 10$ – $20\%$ . Hence, the cost may only be improved by  $\sim 5$ – $10\%$ . Therefore, the focus should not be placed on achieving further energy reductions at higher costs through improved permeability only, but, rather, emphasis should be placed on the critical aspects that offer opportunities to further reduce costs. Such critical aspects include pretreatment and post-treatment analysis and optimization of the performance of RO system that is driven by selectivity, capacity, and flux decline caused by concentration polarization and fouling from inorganic, organic, and biological constituents.<sup>70</sup> Use of a higher-permeability desalination membrane in a RO process that is thermodynamically rather than hydraulically limited<sup>71–75</sup> will be of little commercial benefit because the current state-of-the-art membranes is already enough permeable to meet low-energy needs.

If graphene-based membranes are certainly relevant candidates to be explored for next-generation membranes, it is of paramount importance to critically evaluate the possible impact of graphene-based membranes in the short term by comparing their performance benefits to other materials and with some perspective regarding what the industry needs appear to be today. This is not limiting the future opportunities of a technology in continuous evolution, but only placing this technology in a proper time frame. The most part of the papers we reviewed do not discuss or demonstrate significant improvements in critical aspects such as scaling, fouling, or chemical and thermal stability. This consideration places graphene-based membranes at a quite far in time potential commercial viability. The Lockheed Martin's claims of having developed a membrane that will desalinate water at a fraction of the cost of industry-standard RO systems were criticized by the editor of the *Water Desalination Report*.<sup>76</sup> One of the most critical aspect for their immediate commercialization is scalability. The mass production of large sheets of single-layer graphene films without substantial defects is extremely difficult at present. In addition, nanocomposite membranes are yet very difficult to commercially produce within Quality Assurance/Quality Control requisites. Even if it could be possible to scale it up at a reasonable manufacturing cost and the extremely high permeability is retained, a full-scale plant may not be designed with membranes more permeable than they are today. The fluxes are too high on the front end to follow standard designs, and new plant designs will be needed to commercialize such a high-permeability membrane, which would further delay and add cost to bringing such a membrane to market.

## CONCLUSIONS

Graphene-based membranes have the potentials to become the preferred candidates to next-generation membranes coupling high permeability to high selectivity. However, it is not expected that the uptake of graphene-based membranes may occur in the short term, as industrial membranes employed within current desalination processes must satisfy many additional criteria, and the novel desalination processes needed to take full advantages of the novel membranes are still to be designed. What is needed in the short term are RO membranes that are not simply more permeable and selective, but also chlorine-tolerant, fouling/scaling-tolerant, acid/base-tolerant, easier to clean, and in some applications oil/hydrocarbon- and high temperature-tolerant. The further progress of graphene-based membranes requires a more

systemic approach in addition to basic material research. The design of novel desalination processes is of paramount importance for the uptake of graphene, that otherwise may not deliver the sought improved cost-to-benefit ratios within today's processes.

## ACKNOWLEDGEMENTS

We acknowledge the financial support of the Marie Curie Programme FP7-People-2013-IAAP-WaSClean project No 612250 (S.M. and M.V.) as well as Horizon2020-MSCA-RISE-2016-NANOMED project No. 734641 (M.V.).

## AUTHOR CONTRIBUTIONS:

A.B. and S.C. designed the manuscript, processed the references, prepared the original figures, and wrote the draft manuscript. S.A.-Z., M.V., S.M., and M. Z.A.-A. contributed discussing the manuscript and checking the final version of the manuscript.

## ADDITIONAL INFORMATION

**Competing interests:** The authors declare no competing interests.

**Publisher's note:** Springer Nature remains neutral with regard to jurisdictional claims in published maps and institutional affiliations.

## REFERENCES

1. Water. The United Nations world water development report 2014: water and energy (United Nations, Paris, 2014).
2. Werber, J. R., Osuji, C. O. & Elimelech, M. Materials for next-generation desalination and water purification membranes. *Nat. Rev. Mater.* **1**, 16018 (2016).
3. Boehm, H. P., Clauss, A., Fischer, G. O. & Hofmann, U. Das Adsorptionsverhalten sehr dünner Kohlenstoff-Folien. *Z. Anorg. Allg. Chem.* **316**, 119–127 (1962).
4. Novoselov, K. S. et al. Electric field effect in atomically thin carbon films. *Science* **306**, 666–669 (2004).
5. The Nobel Prize in Physics 2010. [http://www.nobelprize.org/nobel\\_prizes/physics/laureates/2010/](http://www.nobelprize.org/nobel_prizes/physics/laureates/2010/).
6. Lockheed Martin Corporation. Perforene™ membrane. <http://www.lockheedmartin.com/content/dam/lockheed/data/ms2/documents/Perforene-data-sheet.pdf> (2016).
7. Baker, R. W. *Membrane Technology and Applications* (John Wiley & Sons, Hoboken, NJ, USA, 2012).
8. Brodie, B. C. On the atomic weight of graphite. *Philos. Trans. R Soc. Lond.* **149**, 249 (1859).
9. Hummers, W. S. & Offeman, R. E. Preparation of graphitic oxide. *J. Am. Chem. Soc.* **80**, 1339 (1957).
10. Dreyer, D. R., Park, S., Bielawski, C. W. & Ruoff, R. S. The chemistry of graphene oxide. *Chem. Soc. Rev.* **39**, 228–240 (2010).
11. Huang, X. et al. Graphene-based materials: synthesis, characterization, properties, and applications. *Small* **7**, 1876–1902 (2011).
12. Mehta, A. & Zydney, A. L. Permeability and selectivity analysis for ultrafiltration membranes. *J. Memb. Sci.* **249**, 245–249 (2005).
13. Geise, G. M., Paul, D. R. & Freeman, B. D. Fundamental water and salt transport properties of polymeric materials. *Progress. Polym. Sci.* **39**, 1–42 (2014).
14. Amy, G. et al. Membrane-based seawater desalination: Present and future prospects. *Desalination* **401**, 16–21 (2017).
15. Ying, Y. et al. Recent advances of nanomaterial-based membrane for water purification. *Appl. Mater. Today* **7**, 144–158 (2017).
16. Koros, W. J. & Zhang, C. Materials for next-generation molecularly selective synthetic membranes. *Nat. Mater.* **16**, 289–297 (2017).
17. Liu, G., Jin, W. & Xu, N. Graphene-based membranes. *Chem. Soc. Rev.* **44**, 5016–5030 (2015).
18. Xu, Q. & Zhang, W. Next-Generation Graphene-Based Membranes for Gas Separation and Water Purifications. In *Advances in Carbon Nanostructures* (eds Adrian M.T. Silva and Sonia A.C.). (Carabineiro, InTech, London, UK, 2016).
19. Sun, P., Wang, K. & Zhu, H. Recent developments in graphene-based membranes: structure, mass-transport mechanism and potential applications. *Adv. Mater.* **28**, 2287–2310 (2016).
20. Mahmoud, K. A., Mansoor, B., Mansour, A. & Khraisheh, M. Functional graphene nanosheets: the next generation membranes for water desalination. *Desalination* **356**, 208–225 (2015).

21. Cohen-Tanugi, D. & Grossman, J. C. Water desalination across nanoporous graphene. *Nano. Lett.* **12**, 3602–3608 (2012).
22. Surwade, S. P. et al. Water desalination using nanoporous single-layer graphene. *Nat. Nanotechnol.* **10**, 459–464 (2015).
23. Russo, C. J. & Golovchenko, J. A. Atom-by-atom nucleation and growth of graphene nanopores. *Proc. Natl Acad. Sci. USA* **109**, 5953–5957 (2012).
24. O'Hern, S. C. et al. Selective molecular transport through intrinsic defects in a single-layer of CVD graphene. *ACS Nano* **6**, 10130–10138 (2012).
25. O'Hern, S. C. et al. Selective ionic transport through tunable subnanometer pores in single-layer graphene membranes. *Nano. Lett.* **14**, 1234–1241 (2014).
26. O'Hern, S. C. et al. Nanofiltration across defect-sealed nanoporous monolayer graphene. *Nano. Lett.* **15**, 3254–3260 (2015).
27. Cohen-Tanugi, D., Lin, L.-C. & Grossman, J. C. Multi-layer nanoporous graphene membranes for water desalination. *Nano. Lett.* **16**, 1027–1033 (2016).
28. Joshi, R. K. et al. Precise and ultrafast molecular sieving through graphene oxide membranes. *Science* **343**, 752–754 (2014).
29. Nair, R. R., Wu, H. A., Jayaram, P. N., Grigorieva, I. V. & Geim, A. K. Unimpeded permeation of water through helium-leak-tight graphene-based membranes. *Science* **335**, 442–444 (2012).
30. Mi, B. Graphene oxide membranes for ionic and molecular sieving. *Science* **343**, 740–742 (2014).
31. Yeh, C. N., Raidongia, K., Shao, J., Yang, Q. H. & Huang, J. On the origin of the stability of graphene oxide membranes in water. *Nat. Chem.* **7**, 166–170 (2014).
32. Su, Y. et al. Impermeable barrier films and protective coatings based on reduced graphene oxide. *Nat. Commun.* **5**, 4843 (2014).
33. Liu, H., Wang, H. & Zhang, X. Facile fabrication of freestanding ultrathin reduced graphene oxide membranes for water purification. *Adv. Mater.* **27**, 249–254 (2015).
34. Hung, W. S. et al. Cross-linking with diamine monomers to prepare composite graphene oxide framework membranes with varying d-spacing. *Chem. Mater.* **26**, 2983–2990 (2014).
35. Zhang, Y., Zhang, S. & Chung, T. S. Nanometric graphene oxide framework membranes with enhanced heavy metal removal via nanofiltration. *Environ. Sci. Technol.* **49**, 10235–10242 (2015).
36. Nicolai, A., Sumpster, B. G. & Meunier, V. Tunable water desalination across graphene oxide framework membranes. *Phys. Chem. Chem. Phys.* **16**, 8646–8654 (2014).
37. Pawar, P. B., Saxena, S., Badhe, D. K., Chaudhary, R. P. & Shukla, S. 3D oxidized graphene frameworks for efficient nano sieving. *Sci. Rep.* **6**, 21150 (2016).
38. Shen, J. et al. Subnanometer two-dimensional graphene oxide channels for ultrafast gas sieving. *ACS Nano* **10**, 3398–3409 (2016).
39. Akbari, A. et al. Large-area graphene-based nanofiltration membranes by shear alignment of discotic nematic liquid crystals of graphene oxide. *Nat. Commun.* **7**, 10891 (2016).
40. Xu, Z. & Gao, C. Aqueous liquid crystals of graphene oxide. *ACS Nano* **5**, 2908–2915 (2011).
41. Amadei, C. A., Stein, I. Y., Silverberg, G. J., Wardle, B. L. & Vecitis, C. D. Fabrication and morphology tuning of graphene oxide nanoscrolls. *Nanoscale* **8**, 6783 (2016).
42. Zhang, Z., Zou, L., Aubry, C., Jouiad, M. & Hao, Z. Chemically crosslinked rGO laminate film as an ion selective barrier of composite membrane. *J. Membr. Sci.* **515**, 204–211 (2016).
43. Achtyl, J. L. et al. Aqueous proton transfer across single-layer graphene. *Nat. Commun.* **6**, 6539 (2015).
44. Ma, M., Tocci, G., Michaelides, A. & Aeppli, G. Fast diffusion of water nanodroplets on graphene. *Nat. Mater.* **15**, 66–71 (2016).
45. Jiang, Q. et al. Bilayered biofoam for highly efficient solar steam generation. *Adv. Mater.* **28**, 9400–9407 (2016).
46. Azamat, J. Functionalized graphene nanosheet as a membrane for water desalination using applied electric fields: insights from molecular dynamics simulations. *J. Phys. Chem. C* (2016). <https://doi.org/10.1021/acs.jpcc.6b08481>.
47. Burnett, T. L., Yakimova, R. & Kazakova, O. Identification of epitaxial graphene domains and adsorbed species in ambient conditions using quantified topography measurements. *J. Appl. Phys.* **112**, 054308 (2012).
48. Xue, M., Qiu, H. & Guo, W. Exceptionally fast water desalination at complete salt rejection by pristine graphyne monolayers. *Nanotechnology* **24**, 505720 (2013).
49. Kou, J., Zhou, X., Lu, H., Wu, F. & Fan, J. Graphyne as the membrane for water desalination. *Nanoscale* **6**, 1865–1870 (2014).
50. Zhu, C., Li, H., Zeng, X. C., Wang, E. G. & Meng, S. Quantized water transport: ideal desalination through graphyne-4 membrane. *Sci. Rep.* **3**, 3163 (2013).
51. Lin, L.-C., Choi, J. & Grossman, J. C. Two-dimensional covalent triazine framework as an ultrathin-film nanoporous membrane for desalination. *Chem. Commun.* **51**, 14921–14924 (2015).
52. Heiraniyan, M., Farimani, A. B. & Aluru, N. R. Water desalination with a single-layer MoS<sub>2</sub> nanopore. *Nat. Commun.* **6**, 8616 (2015).
53. Garnier, L., Szymczyk, A., Malfreyt, P. & Ghoufi, A. Physics behind water transport through nanoporous boron nitride and graphene. *J. Phys. Chem. Lett.* **7**, 3371–3376 (2016).
54. Livingston, A. G. *Metal Organic Frameworks (MOFs) in Membranes for Organic Solvent Nanofiltration*. (2014 Annual NAMS Conference, Houston, TX, 2014).
55. Agre, P. et al. Aquaporin water channels- from atomic structure to clinical medicine. *J. Physiol.* **542**, 3–16 (2002).
56. Peter, C. & Hummer, G. Ion transport through membrane-spanning nanopores studied by molecular dynamics simulations and continuum electrostatics calculations. *Biophys. J.* **89**, 2222–2234 (2005).
57. Holt, J. K. et al. Fast mass transport through sub-2-nanometer carbon nanotubes. *Science* **312**, 1034–1037 (2006).
58. Liu, L. et al. Graphene oxidation: thickness-dependent etching and strong chemical doping. *Nano. Lett.* **8**, 1965–1970 (2008).
59. Robertson, B. C. & Zydney, A. L. Protein adsorption in asymmetric ultrafiltration membranes with highly constricted pores. *J. Colloid Interface Sci.* **134**, 563–575 (1990).
60. Marin, A., Khan, Z., Zaidi, S. M. J. & Boyce, M. C. Biofouling in reverse osmosis membranes for seawater desalination: phenomena and prevention. *Desalination* **281**, 1–16 (2011).
61. Vert, M. et al. Terminology for biorelated polymers and applications (IUPAC Recommendations 2012). *Pure. Appl. Chem.* **84**, 377–410 (2012).
62. Guillen, G. & Hoek, E. M. V. Modeling the impacts of feed spacer geometry on reverse osmosis and nanofiltration processes. *Chem. Eng. J.* **149**, 221–231 (2009).
63. Li, L., Dong, J., Nenoff, T. M. & Lee, R. Desalination by reverse osmosis using MFI zeolite membranes. *J. Membr. Sci.* **243**, 401–404 (2004).
64. Li, L., Dong, J. & Nenoff, T. M. Transport of water and alkali metal ions through MFI zeolite membranes during reverse osmosis. *Sep. Purif. Technol.* **53**, 42–48 (2007).
65. Liu, N., Li, L., McPherson, B. & Lee, R. Removal of organics from produced water by reverse osmosis using MFI-type zeolite membranes. *J. Membr. Sci.* **325**, 357–361 (2008).
66. Lind, M. L., Eumine Suk, D., Nguyen, T. V. & Hoek, E. M. Tailoring the structure of thin film nanocomposite membranes to achieve seawater RO membrane performance. *Environ. Sci. Technol.* **44**, 8230–8235 (2010).
67. Kumar, M., Grzelakowski, M., Zilles, J., Clark, M. & Meier, W. Highly permeable polymeric membranes based on the incorporation of the functional water channel protein Aquaporin Z. *Proc. Natl Acad. Sci. USA* **104**, 20719–20724 (2007).
68. Corry, B. Designing carbon nanotube membranes for efficient water desalination. *J. Phys. Chem. B.* **112**, 1427–1434 (2008).
69. Pendergast, M. M. & Hoek, E. M. A review of water treatment membrane nanotechnologies. *Energy Environ. Sci.* **4**, 1946–1971 (2011).
70. Imbrogno, J., Keating, J. J., Kilduff, J. & Belfort, G. Critical aspects of RO desalination: a combination strategy. *Desalination* **401**, 68–87 (2017).
71. Song, L. et al. Performance limitation of the full-scale reverse osmosis process. *J. Membr. Sci.* **214**, 239–244 (2003).
72. Zhou, W., Song, L. & Guan, T. K. A numerical study on concentration polarization and system performance of spiral wound RO membrane modules. *J. Membr. Sci.* **271**, 38–46 (2006).
73. Zhu, A., Rahardianto, A., Christofides, P. D. & Cohen, Y. Reverse osmosis desalination with high permeability membranes-cost optimization and research needs. *Desalin. Water Treat.* **15**, 256–266 (2010).
74. Zhu, A., Christofides, P. D. & Cohen, Y. Effect of thermodynamic restriction on energy cost optimization of RO membrane water desalination. *Ind. Eng. Chem. Res.* **48**, 6010–6021 (2008).
75. Rahardianto, A., Gao, J., Gabelich, C. J., Williams, M. D. & Cohen, Y. High recovery membrane desalting of low-salinity brackish water: integration of accelerated precipitation softening with membrane RO. *J. Membr. Sci.* **289**, 123–137 (2007).
76. Graphene membrane technology update. Water Desalination Report. Global Water Intelligence, a Media Analytics Ltd. Company 2014. <https://www.desalination.com/issues/2420> (2017).



**Open Access** This article is licensed under a Creative Commons Attribution 4.0 International License, which permits use, sharing, adaptation, distribution and reproduction in any medium or format, as long as you give appropriate credit to the original author(s) and the source, provide a link to the Creative Commons license, and indicate if changes were made. The images or other third party material in this article are included in the article's Creative Commons license, unless indicated otherwise in a credit line to the material. If material is not included in the article's Creative Commons license and your intended use is not permitted by statutory regulation or exceeds the permitted use, you will need to obtain permission directly from the copyright holder. To view a copy of this license, visit <http://creativecommons.org/licenses/by/4.0/>.